https://doi.org/10.5194/egusphere-2026-3156
Preprint. Discussion started: 11 June 2026

Inferring heating and cooling rates at the MLT from multistatic meteor radar observations and intercomparison to SE-WACCM-X and JAWARA

Gunter Stober[1,2], Hanli Liu[3], Zishun Qiao[3], Kaoru Sato[4], Loretta Pearl Poku[1,2], Witali Krochin[1,2], Alan Liu[5], Alexander Kozlovsky[6], Diego Janches[7], Jie Zeng[8,9,10], Wen Yi[8,9,10], Masaki Tsutsumi[11,12], Njål Gulbrandsen[13], Satonori Nozawa[14], Mark Lester[15], Johan Kero[16], and Nicholas Mitchell[17,18]

[1]Institute of Applied Physics, University of Bern, Switzerland
[2]Oeschger Center for Climate Change Research, University of Bern, Switzerland
[3]High Altitude Observatory, NSF National Center for Atmospheric Research, Boulder, Colorado, USA
[4] Department of Earth and Planetary Science, University of Tokyo, Tokyo, Japan
[5]Center for Space and Atmospheric Research, Department of Physical Sciences, Embry-Riddle Aeronautical University, Daytona Beach, Florida, USA
[6]Sodankylä Geophysical Observatory, University of Oulu, Oulu, Finland
[7]ITM Physics Laboratory, Mail Code 675, NASA Goddard Space Flight Center, Greenbelt, MD 20771, USA
[8]National Key Laboratory of Deep Space Exploration, School of Earth and Space Sciences, University of Science and Technology of China, Hefei 230026, China
[9]CAS Center for Excellence in Comparative Planetology, University of Science and Technology of China, Hefei, China
[10]Anhui Mengcheng National Geophysical Observatory and Research Station, School of Earth and Space Sciences, University of Science and Technology of China, Hefei, China
[11]National Institute of Polar Research, Tachikawa, Japan
[12]The Graduate University for Advanced Studies (SOKENDAI), Tokyo, Japan
[13]Tromsø Geophysical Observatory UiT – The Arctic University of Norway, Tromsø, Norway
[14]Institute for Space-Earth Environmental Research, Nagoya University, Japan
[15]Department of Physics and Astronomy, University of Leicester, Leicester, UK
[16]Swedish Institute of Space Physics (IRF), Kiruna, Sweden
[17]British Antarctic Survey, Cambridge, UK
[18]Department of Physics and Astronomy, University of Leicester, Leicester, UK

Correspondence: Gunter Stober (gunter.stober@unibe.ch)

Abstract. Continuous measurements of vertical wind in the mesosphere and lower thermosphere are rare and technically challenging. However, multistatic meteor radar networks, such as the Nordic Meteor Radar Cluster, offer a unique opportunity to use advanced tomographic wind retrieval methods to determine neutral winds, including vertical wind components. The Spherical Volume Velocity Processing technique is a newly developed tomographic algorithm that enables the extraction of Doppler-based vertical winds and the computation of vertical winds from horizontal divergence through vertical integration. In this study, we present an intercomparison of various vertical wind retrieval methods to evaluate remaining biases and to quantify the magnitude of summer mesospheric vertical upwelling and corresponding downwelling. The retrieved wind data are compared with the Japanese meteorological reanalysis known as JAWARA, as well as a year of free-running SE-WACCM-X model data. Our findings indicate a strong agreement concerning the seasonal patterns of horizontal winds between the Nordic Meteor Radar Cluster and both models. The observed vertical wind velocities range from 2 to 15 cm/s. Additionally,

https://doi.org/10.5194/egusphere-2026-3156
Preprint. Discussion started: 11 June 2026

measurements from the Nordic Meteor Radar Cluster show cooling and heating rates of -40 to 100 K/day during summer and 5 to 20 K/day in the winter months.

1 Introduction

Gravity waves play a crucial role in the energetic state of the mesosphere/lower thermosphere. They drive a meridional flow, which causes a summer hemispheric upwelling and winter downwelling at mid- and polar latitudes. This residual circulation is associated with vertical motions resulting in adiabatic cooling or heating, forcing the thermal equilibrium temperature up to 100 K away from its radiatively determined balance (Lindzen, 1981; Smith, 2012; Becker, 2012). However, the vertical velocities induced by this circulation are rather small, posing challenges in measuring the hemispheric summer/winter upwelling/downwelling and corresponding cooling/heating rates. General Circulation Models (GCMs) predicted values for the mesospheric summertime upwelling in the order of a few cm/s.

In the past, vertical wind measurements were often limited to short campaigns with expensive HPLA aperture radars (Fritts et al., 1990; Hoppe and Fritts, 1995a). These measurements showed vertical velocities in the opposite direction from what was expected from theory. Simpler systems, such as MAARSY, were able to perform nearly continuous soundings but did depend on some form of mesospheric scatterers such as polar mesospheric summer echoes (Sommer et al., 2016; Stober et al., 2018b; Gudadze et al., 2019). However, these measurements indicated that the scatterer physics plays a leading role and is hard to discriminate from the neutral wind. However, PMSE observations with PANSY (Sato et al., 2014) indicated that GW frequency spectra of horizontal and vertical winds resulted in values required to simulate realistic zonal wind fields in GCMs (Sato et al., 2017). More recently, Chu, Xinzhao et al. (2026) presented several hours of vertical winds measured over McMurdo using an Iron Boltzmann Lidar system. These vertical winds did show a short-term variability of ± 3 m/s, but the measurements were not long enough to derive a seasonal mean vertical velocity. However, the most important aspect of the lidar data is the constraint on the magnitude of the short-term variability within the small (tiny) sensor volume of the lidar beam on time scales of minutes, which resolves the full temporal GW spectrum up to the Brund-Väisälä frequency and also down to the smallest spatial scales. Previous attempts using monostatic meteor radars or multistatic meteor radar networks resulted in very large vertical velocities of several m/s for successive days or up to 1 m/s for the whole year (Egito et al., 2016; Chau et al., 2017). These large values and systematic biases are related to the sliding of the Bragg vector along the trail while it is advected by horizontal winds, resulting in substantial apparent vertical velocities (Stober et al., 2022). Furthermore, meteor radars are calibrated in phase to achieve angular precisions of 2° for their interferometric solution. Additional pointing errors are related to aging antennas or ground plane conditions that can alter the pointing slightly (Zeng et al., 2022), introducing tiny projection errors that result in systematic biases of the derived vertical winds.

In this study, we will derive constraints on the magnitude of the seasonal pattern of vertical winds using a newly developed

https://doi.org/10.5194/egusphere-2026-3156
Preprint. Discussion started: 11 June 2026

Spherical Volume Velocity Processing SVVP (Poku et al., 2026). The retrieval is applied to multistatic meteor radar observations above Fennoscandia using four meteor radars belonging to the Nordic Meteor Radar Cluster. The new retrieval is tested at temporal resolutions of 15 minutes and 30 minutes to estimate the sensitivity of the temporal resolution on the vertical wind climatology. Furthermore, the SVVP algorithm obtains measurements of the horizontal divergence, which are used to estimate a divergence-based vertical wind estimate, which solely depends on horizontal winds and, thus, provides independent information on the vertical velocity. We perform a climatological comparison of zonal, meridional, and vertical winds to our observations with a free run of SE-WACCM-X (Liu et al., 2024) and the Japanese meteorological reanalysis JAWARA (Sato et al., 2023; Sato and Koshin, 2025) for the period from 2021 until the end of 2025.

The manuscript is structured as follows. Section 2 presents a technical summary of the Nordic Meteor Radar Cluster, while sections 3 and 4 present briefly the JAWARA and SE-WACCM-X models, respectively. The results for the horizontal winds, an intercomparison of the different retrieved vertical winds, the bias correction, and the heating and cooling rates are shown in Section 5. The inter-year differences are discussed in Section 6. Section 7 presents a discussion of key aspects of our analysis and also the remaining issues of the techniques. We summarize the results in the conclusion section.

2 Nordic Meteor Radar Cluster

The Nordic Meteor Radar Cluster (NMRC) consists of six meteor radars in Fennoscandia and on the island of Svalbard. The MRs are located at Tromsø (69.59^o N, 19.2^o E; TRO), Trondheim (63.41^o N, 10.47 ^{o} E; TDH), Alta (70.0^o N, 23.3^o E; ALT), Sodankylä (67.4^o N, 26.6^o E; SOD), Kiruna (67.9^o N, 21.1^o E; KIR), Svalbard (78.2^o N, 16.0^o E; SVA). In this study, we focus on the mainland systems with overlapping observation volumes to apply multistatic inversion algorithms to infer reliable seasonal horizontal and vertical winds. Data from the Svalbard MR and Trondheim MR were not included in the analysis. The Trondheim MR was refurbished in May 2025 and is now back in operation.

Reliable vertical wind measurements require continuous data collection. In September 2021, the Tromsø MR was updated with new receiver hardware, and data acquisition was brought to the latest software standard for ATRAD systems. The Kiruna MR was also refurbished and resumed operation with the new hardware on 18th March 2024 at 11:50 UTC. We cross-checked the system performance before and after to ensure that no obvious bias was introduced related to the interferometric solution, range sampling, and background noise. However, in both cases, spurious detections were reduced, and the number of meteor detections increased, resulting in an improved measurement response (smaller statistical uncertainties). For the multistatic analysis, we only used data collected between 2021 and the end of 2025 from Tromsø, Alta, Kiruna, and Sodankylä. Figure 1 shows a map with the location of all radars on the mainland. In Table 1, we summarize the experimental parameters and the changes that were implemented in Kiruna.

The winds are computed with the Spherical Volume Velocity Processing (SVVP) that was introduced in Poku et al. (2026). The algorithm includes full non-linear error propagation for the mean winds and angular uncertainties, and accounts for variable spatial and temporal sampling (Stober et al., 2018a; Gudadze et al., 2019). Furthermore, we have to emphasize that the line-of-sight velocities are corrected for the specular geometry, resulting in apparent vertical motions due to the sliding of the

https://doi.org/10.5194/egusphere-2026-3156
Preprint. Discussion started: 11 June 2026

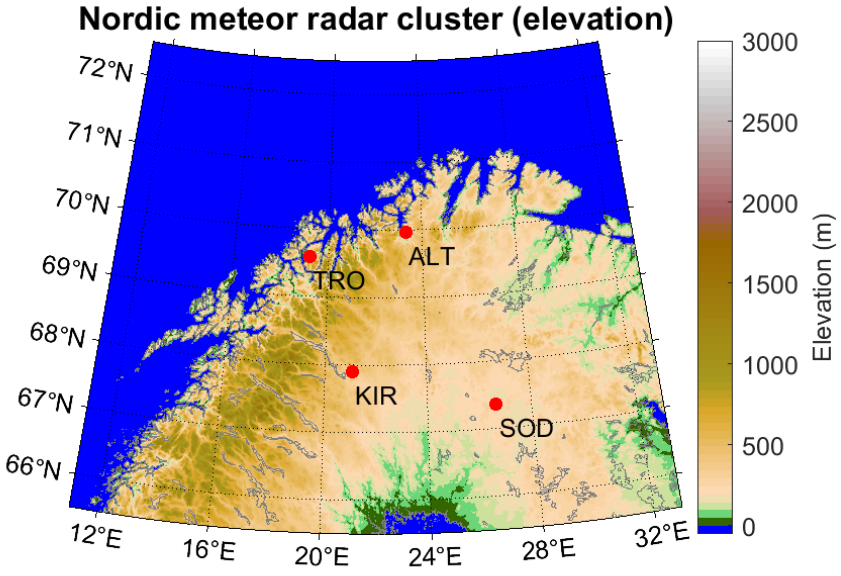

Figure 1. Nordic Meteor Radar Cluster locations at TRO, ALT, KIR, and SOD (red dots). The plot is generated with etopo1 using the m_map package (Amante and Eakins, 2009).

	Frequency (MHz)	Peak Power (kW)	PRF (Hz)	Coherent Integrations	Pulse Form/Code	Sampling (km)
TRO	30.25	7.1	400	4	4-bit complementary	1.5
ALT	31.00	10.1	440	4	4-bit complementary	1.8
KIR	32.55	6/15	2144/625	4	mono/7-bit Barker	2/1.5
SOD	36.90	7.5/15	2144	4	mono	2

Table 1. Operational Parameters of the NORDIC Meteor Radar Cluster network. PRF describes the Pulse Repetition Frequency. The MR located at Kiruna was updated on 18th March 2024 and has been operating with new experiment parameters since then. In September 2009, the Sodankylä MR was upgraded to a 15 kW transmitter.

scattering center along the trail (Stober et al., 2022). We apply a mean correction for all systems due to the lack of exact and precise trajectory information for each detected meteor for all systems of the network.

3 JAWARA

The JAGUAR-DAS whole nuetal atmosphere reanalysis (JAWARA) provides meteorological fields of temperature, three-dimensional wind, geopotential height, temperature tendency from diabatic heating, zonal and meridional forcings from gravity wave parameterizations (Sato and Koshin, 2025; Koshin et al., 2025). The reanalysis assimilates observations from the mete-

https://doi.org/10.5194/egusphere-2026-3156
Preprint. Discussion started: 11 June 2026

orological PrepBUFR of temperature, horizontal wind, relative humidity, and surface pressure from 0-30 km altitude. At the stratosphere and mesosphere, AURA MLS (sun-synchronous) and TIMED SABER (non-sun synchronous) temperatures are assimilated together with brightness temperatures from DMSP SSMIS satellites. Details on the data assimilation schemes are found in Koshin et al. (2020, 2022). An intercomparison of JAWARA with MERRA2, NAVGEM-HA, and WACCMX-DART is presented in McCormack et al. (2021).

4 SE-WACCM-X

The Whole Atmosphere Community Climate Model with thermosphere/ionosphere extension (WACCM-X) is a well-known comprehensive model covering the entire atmosphere up to the thermosphere and is part of the Community Earth System Model (Liu et al., 2018). WACCM-X still relies on gravity wave parameterizations; non-orographic gravity waves are based on the approach from Garcia et al. (2017); Richter et al. (2010), and orographic waves are parameterized according to McFarlane (1987). There is also a specified dynamics version, called SD-WACCM-X, which is nudged to MERRA2 reanalysis (Gelaro et al., 2017) up to 60 km in altitude. However, even nudged to reanalysis at the stratosphere and with decreasing nudging strength at the lower mesosphere, the resulting wind at the MLT region showed characteristic seasonal effects deviating from observations(Stober et al., 2021; Hindley et al., 2022), which were attributed to the GW parameterizations.

In this study, we analyzed three-dimensional winds obtained with the SE-WACCM-X version. This version builds on a spectral elements dynamical core (Lauritzen et al., 2018), instead of the finite volume dynamical core of WACCM-X. The spectral elements dynamical core permits running SE-WACCM-X at a much higher spatial resolution, omitting some of the GW parameterizations, improving horizontal winds, and also vertical transport (Liu, 2025). Horizontal and vertical winds are analyzed using a SE-WACCM-X run with NE120/L273 configuration, reaching an effective 25km spatial resolution with a vertical resolution of 0.1 scale heights. More details about SE-WACCM-X can be found in Liu et al. (2024).

5 Results

5.1 Horizontal wind climatologies

Both models undergo a similar data reduction pipeline. We select the same reference coordinate as for the Nordic Meteor Radar Cluster SVVP algorithm (22° E, 69° N) and average all points that fall within a circle of 250 km in radius to obtain the mean horizontal winds. A similar procedure was already implemented in a previous MR wind model intercomparison (Stober et al., 2021). The coarser spatial resolution of JAWARA plays only a minor role during the data reduction to calculate the zonal and meridional wind climatology.

Daily mean wind climatologies for SE-WACCM-X are based on a one-year free run with a temporal resolution of 6 hours. Seasonal zonal and meridional daily mean wind climatologies are obtained using a 30-day running boxcar with periodic boundary conditions. The 30-day window acts as a low-pass filter and removes most of the short-term variability due to planetary waves, tides, and gravity waves. Geopotential heights have been converted into geometric altitudes using the WGS84 system to calcu-

https://doi.org/10.5194/egusphere-2026-3156
Preprint. Discussion started: 11 June 2026

late Earth's radius at our reference coordinate.

JAWARA reanalysis is available for the same period as the Nordic Meteor Radar Cluster SVVP winds from January 2021 until December 2025. JAWARA data has an hourly temporal resolution. The geopotential latitudes are processed similarly to SE-WACCM-X to obtain geometric altitudes. Daily mean zonal and meridional winds are obtained from the domain-averaged hourly reanalysis data, applying the Adaptive spectral filter with vertical tidal phase regularization (ASF2D) (Stober et al., 2020, 2021). Seasonal zonal and meridional wind climatologies are calculated by averaging the same day of the year and averaging the resulting time series with a 30-day boxcar with periodic boundary conditions.

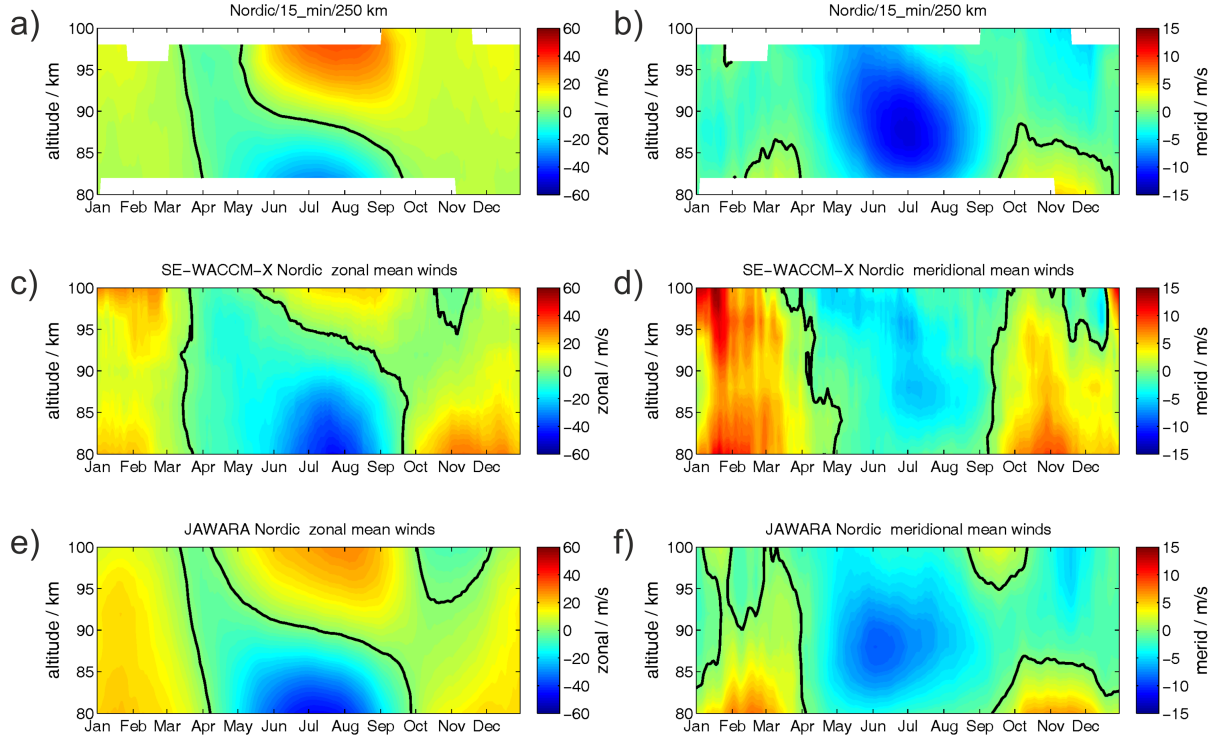

Figure 2. Comparison of zonal and meridional winds between the Nordic Meteor Radar Cluster (upper row, panels a) and b)), the free-running SE-WACCM-X (central row, panels c) and d)), and the JAWARA reanalysis (lower row, panels e) and f)).

Figure 2 shows a comparison of the zonal and meridional mean wind climatologies obtained from the NMRC (upper row), SE-WACCM-X (central row), and JAWARA (lower row). Zonal winds exhibit moderate to weak eastward winds during the hemispheric winter season between 80-100 km altitude in all data sets. The spring transition and summer zonal wind reversal are also well-reproduced from SE-WACCM-X and JAWARA. The seasonal asymmetry and gradual descent of the zonal wind reversal altitude are captured by both models compared to the NMRC measurements. However, SE-WACCM-X has a tendency to show the reversal altitude at a bit higher altitudes compared to the NMRC measurements and JAWARA. Only the magni-

https://doi.org/10.5194/egusphere-2026-3156
Preprint. Discussion started: 11 June 2026

tudes of the zonal eastward and westward jets indicate some offset. Around November, JAWARA and SE-WACCM-X exhibit again a zonal reversal altitude above 95 km, which is absent in the observations. Merdional winds exhibit a similar seasonal morphology with southward winds during the hemispheric summer and northward winds during the winter season. Due to the much smaller magnitude of the mean zonal wind, there are some discrepancies in the meridional wind reversal altitudes during the winter season compared to the observations. However, both models have a tendency to underestimate the meridional summer southward wind jet that corresponds to the zonal wind reversal altitude during the summer season.

5.2 Vertical wind analysis Nordic

MLT seasonal mean vertical winds belong to the most challenging parameters that can be inferred from remote sensing data. Models predict mean values for the summer upwelling of a few cm/s and a winter downwelling, which is even smaller. Given these small numbers, it is crucial to remove all potential offsets intrinsic to the observations related to the geometric effects of the sensor and the tracer. MRs have been in operation for decades, but so far, reliable vertical wind measurements have been out of reach. The recently implemented SVVP presents a new pathway to constrain vertical winds at the MLT by using multistatic MR observations (Poku et al., 2026).

Our implementation of the SVVP algorithm offers two possibilities to estimate vertical wind velocities. The first method is related to the direct Doppler measurement w and is directly fitted in the SVVP; the other approach integrates the derived horizontal divergence to infer a relative vertical wind velocity profile w_{div};

$$\Delta w = \int_{z_1}^{z_2} div \cdot v_h \; dz \quad . \tag{1}$$

Here is Δw, the relative change of the vertical wind between two vertical layers, $div \cdot v_h$ is the horizontal divergence, and dz denotes the width of the vertical layer. However, the obtained profile depends on an initial value at the upper or lower edge, which is a priori unknown and needs to be determined. We will refer to this procedure as calibration and bias correction. We compute a vertical wind profile for each time step and determine a mean vertical wind bias over the entire layer between 80 and 100 km so that the mean vertical motion over the 20 km layer vanishes.

Considering the approaches presented in Rodgers (2000), we can use additional information for the calibration procedure. The most precise and accurate information about the long-term vertical motion of the MLT is provided by measuring the meteor ablation altitude (Clemesha and Batista, 2006; Stober et al., 2014; Yi et al., 2018; Dawkins et al., 2023, 2024). Typical altitude variations over a solar cycle are in the order of -10 to -817 m/dec. This corresponds to a mean vertical motion over the entire meteor layer from 80-100 km of about $-2.6 \cdot 10^{-4} cm/s$. Considering the magnitude of the number, it is justified to assume that the mean vertical velocity over one year is essentially zero.

Doppler-retrieved vertical winds use the mathematical approach with a generalized Tikhonov regularization as presented in Stober et al. (2022). This technique mainly cures for the scattering effect of the sliding Bragg vector along the trail while the trail is advected by horizontal winds, resulting in an inflation of the vertical component and thus an apparent vertical wind velocity. This correction is based on empirical geometries, as we have no information about the trajectory for each meteor. Fur-

https://doi.org/10.5194/egusphere-2026-3156
Preprint. Discussion started: 11 June 2026

thermore, the regularization strength is controlled by the statistical uncertainties and measurement statistics. Thus, at altitudes with only a few meteor detections, the Tikhonov regularization dominates, and the vertical wind stays around zero.

Furthermore, the expected mean vertical winds are so small that we also need a seasonal debiasing. Doppler-retrieved vertical winds are very sensitive to any kind of systematic error in the interferometry or systematic geometric effects inside the NMRC. The seasonal de-biasing helps to mitigate these residual errors due to potential small errors in the antenna pointing for each of the 4 radars. We have checked the interferometric solution by tracking meteor showers with all 4 systems and found differences of up to 2 °. Furthermore, we assume that there are no systematic pointing errors between the radars.

In Figure 3, we present seasonal climatologies of Doppler-retrieved and horizontal divergence-derived vertical winds for temporal resolutions of 15 and 30 minutes. The left column shows the Doppler-retrieved winds, and the right column presents the horizontal divergence vertical integrate vertical winds. Independent of the method, all vertical winds show a similar seasonal pattern with an upwelling during the summer months and a weak downwelling during the hemispheric winter season. Furthermore, the Doppler-retrieved winds indicate the edge effects and are only reliable between 84-95 km, the altitude where most of the specular meteors are detected, as well as scaling with the temporal resolution. The magnitude of the horizontal divergence-based vertical winds exceeds the values of the Doppler-retrieved winds by 25-50%. However, the temporal resolution dependency is much weaker. We also calculated the values for a 60-minute temporal resolution, which resulted in horizontal divergence based on vertical winds between the 15 and 30 minute values, indicating that these winds are almost independent of the temporal resolution. A crucial aspect of the derived vertical wind climatologies is the seasonal de-biasing.

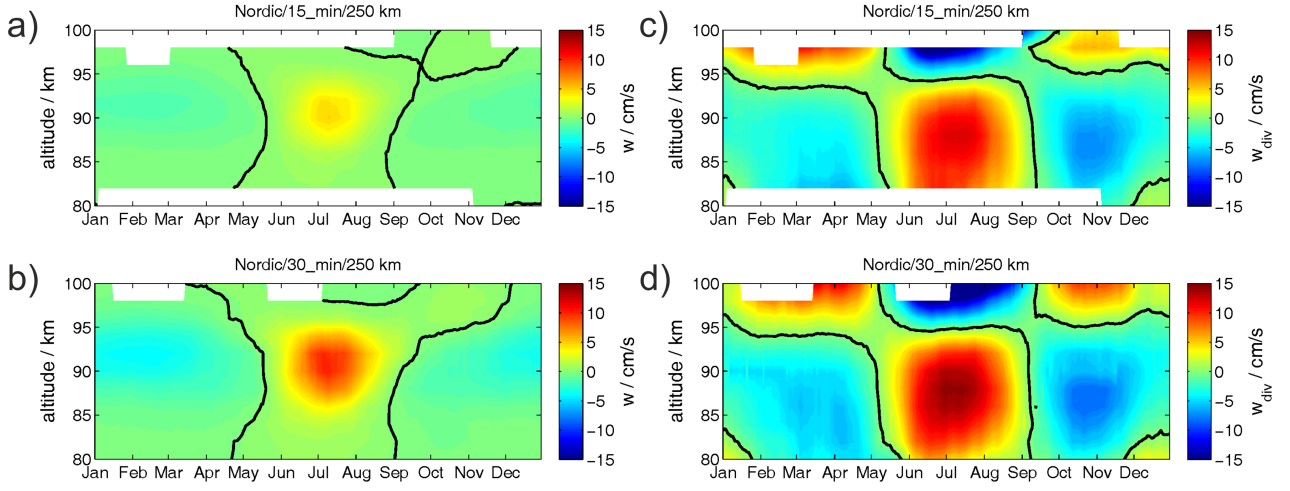

Figure 3. Comparison of vertical wind climatologies for the NMRC using a temporal resolution of 15 and 30 minutes. Panels a) and b) show the Doppler-retrieved vertical wind for both temporal resolutions, panels c) and d) present the corresponding horizontal divergence-derived vertical wind for both temporal resolutions, respectively.

Figure 4 presents the seasonal altitude-dependent bias for 15 and 30 minutes. The scaling behaviour of the bias with temporal resolution points towards sampling effects. The 15-minute resolution winds resolve more scales of the GW spectrum but suffer

https://doi.org/10.5194/egusphere-2026-3156
Preprint. Discussion started: 11 June 2026

from the much sparser sampling, whereas the 30-minute average already misses some of the small-scale fluctuations, which are known to produce the largest vertical wind fluctuations (Chu, Xinzhao et al., 2026). Furthermore, we show a normalized altitude distribution. The mean seasonal bias for the Doppler-retrieved and horizontal divergence-inferred vertical winds is nearly identical for the 15-minute temporal resolution and shows a moderate agreement for the 30-minute temporal resolution. The magnitude of the bias is, in the case of the horizontal divergence-based vertical wind, in the order of a few cm/s and much smaller than the total magnitude. The 30-minute Doppler-retrieved vertical winds also show increased bias at the altitudes with the best measurement statistics, suggesting that residual pointing errors and our empirical scattering correction may still have an impact.

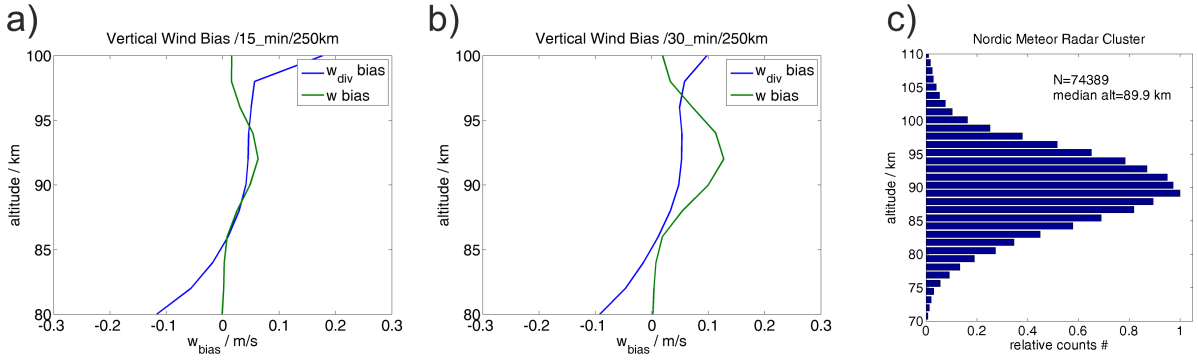

Figure 4. Vertical wind seasonal bias for 15 and 30 minute temporal resolution is shown in panels a) and b), respectively. A normalized altitude distribution is visualized in panel c) for comparison as a proxy of the measurement statistics.

SVVP-derived vertical winds seem to reflect a realistic seasonal morphology and permit setting limits for the vertical wind magnitudes. The 15-minute Doppler-derived winds present the lower limit, whereas the divergence-inferred vertical winds provide an upper boundary for the climatological analysis.

5.3 Validity of Incompressibility Assumption

A crucial aspect of horizontal divergence-inferred vertical winds is the validity of the incompressibility assumption. A flow is considered incompressible when the Mach number is below 0.3. Velocities exceeding a speed of Mach 0.3 are called subsonic flow, and compressibility effects have to be taken into account. However, the threshold of Mach 0.3 is not a singularity, and compressibility effects already occur below, but are usually considered small and often neglected. We estimated the Mach number using the total wind speeds from the SVVP analysis and the JAWARA temperature climatology. The specific heat ratio γ was assumed to be 1.4. We estimated the Mach number for the mean winds and for the diurnal max wind.

Figure 5 shows the Mach numbers for the daily mean flow velocity and the diurnal maximum velocity for both temporal resolutions, respectively. The calculated Mach numbers indicate that the daily mean flow velocity is typically far away from the 0.3 Mach threshold and, thus, the mean flow can be assumed to be incompressible. However, considering the maximum velocities at temporal scales of hours and minutes, the flow speed can well exceed Mach 0.3, and compressibility effects become

https://doi.org/10.5194/egusphere-2026-3156
Preprint. Discussion started: 11 June 2026

relevant. In particular, atmospheric tides can have large enough amplitudes to reach Mach numbers above 0.3. Individual measurements show Mach numbers of beyond 0.5 Mach. The highest Mach numbers seem to occur during the hemispheric summer months at all altitudes and during the winter above 90-95 km altitude. During the Hunga Tonga eruption, the CONDOR radar recorded wind speeds of above 200 m/s corresponding to Mach 0.85-0.9 (Qiao et al., 2025; Stober et al., 2023).

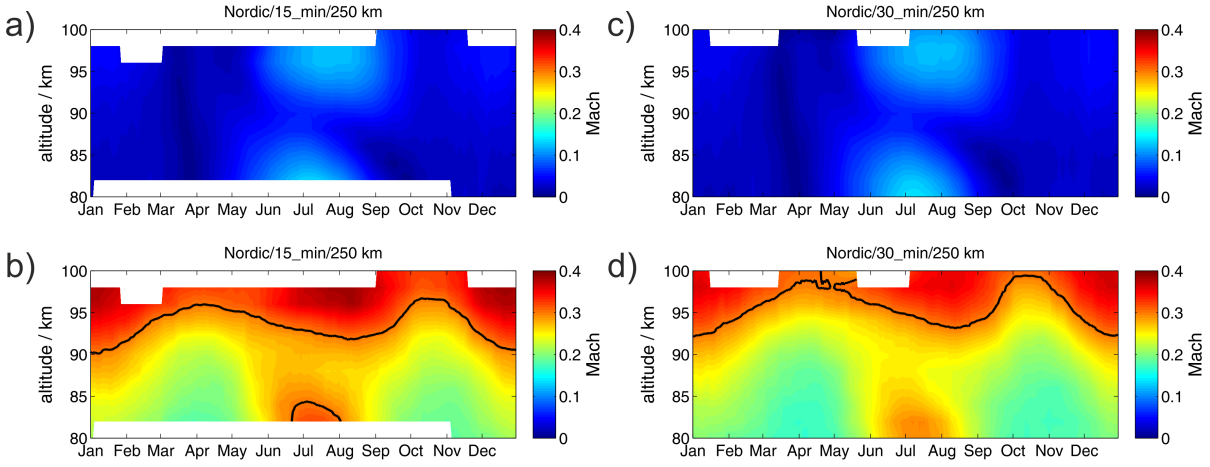

Figure 5. Calculated Mach numbers for mean total winds a) with 15-minute temporal resolution and c) 30-minute temporal resolution. Panels b) and d) show the Mach number of the diurnal maximum velocity and both temporal resolutions, respectively.

The relative importance of compressibility effects due to small-scale GWs was already discussed in Stober et al. (2022). A scale analysis based on linear theory (Fritts and Alexander, 2003) indicated that the incompressibility assumption causes an error of 3-4% for most resolved GWs. However, Vadas (2013) derived the polarization and dispersion relation of GW for compressible flows and demonstrated that the effect plays a crucial role for deep primary GWs with long vertical wavelengths, e.g., GWs generated in convective plumes (Vadas, 2013) and secondary GWs (Vadas et al., 2018). Thus, the vertical winds derived from the horizontal divergence present only an upper limit, and the true winds are likely smaller. The compressibility effect is not canceled out when averaged over tidal phases, and results in an overestimation of horizontal divergence. Even if the flow speed during a tidal phase remains incompressible, it might become compressible during the other phase. So there is a remaining net effect on the horizontal divergence.

5.4 Vertical wind climatological comparison

JAWARA and SE-WACCM-X use pressure as a vertical coordinate and, thus, vertical winds are provided in pressure coordinates $\omega(Pa/s)$. Thus, we convert the pressure-based vertical wind into geometric coordinates using the WGS84 coordinate system. We estimate the altitude-dependent scale height H as a function of temperature and Earth's gravitational constant g.

https://doi.org/10.5194/egusphere-2026-3156
Preprint. Discussion started: 11 June 2026

The vertical winds are then obtained by the simple conversion:

$$w = -\frac{\omega}{p} \cdot H \quad . \tag{2}$$

Here, p denotes the pressure, and w is the vertical velocity in WGS84 altitude. Vertical wind climatologies were computed for SE-WACCM-X and JAWARA following the procedure for the horizontal winds.

Figure 6 shows the derived climatologies for SE-WACCM-X and JAWARA in comparison to the SVVP inferred vertical

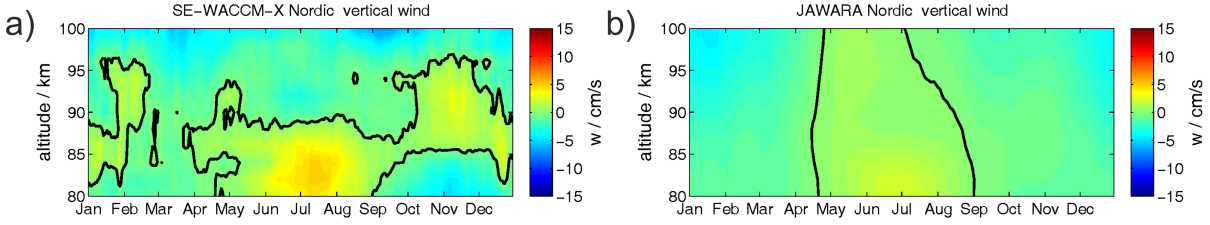

Figure 6. Comparison of vertical wind climatologies in (a) free-running SE-WACCM-X, and (b) JAWARA reanalysis.

winds measured by the NMRC. The NRMC observations and both models exhibit a summertime upwelling and hemispheric winter downwelling. The black contour indicates the zero line transition. Although there are still some magnitude differences in the vertical velocities, the seasonal morphology and general structure are reproduced by either method. Furthermore, SE-WACCM-X seems to generate a stronger summer mesopause upwelling compared to JAWARA. The magnitude of the summer upwelling in SE-WACCM-X almost agrees with the NMRC observations (15 min resolution). Only the altitude of the maximum upwelling during the summer seems to be a bit lower in SE-WACCM-X. It is also remarkable that there is a kind of T-shape in the vertical winds showing an upward motion during fall and the spring transition in the observations, which is also found to some degree in SE-WACCM-X. JAWARA appears to show less vertical structure and only reflects a clear seasonal behavior without a distinct maximum that can be associated with the summertime wind reversal.

5.5 Heating and cooling rates

Vertical winds play a crucial role in the summer mesopause temperature and energy balance, therefore we calculate the heating/cooling rates. Unrealistically high vertical upwelling would result in extreme cooling rates, which would require a heat source at the MLT to maintain a stable balance. We estimate the heating/cooling rates by calculating a mean vertical velocity from 86-94 km. SE-WACCM-X vertical winds are averaged between 80-90 km to capture the maximum summer upwelling. We applied the same altitude kernel for JAWARA. This is the height region with the most reliable vertical winds from the NMRC. Furthermore, the adiabatic temperature gradient is derived at an altitude of 90 km, accounting for reduced Earth gravity. The heating/cooling rates are then estimated by assuming only vertical motion (Yue and Wang, 2025).

The resulting mean vertical winds and corresponding heating/cooling rates are shown in Figure 7. NMRC observations and both models again show the same seasonal pattern in the vertical winds and also in the heating/cooling rates. The grey shaded area denotes the variability for the models and includes a full error propagation for the measurements. The 30-minute NMRC

https://doi.org/10.5194/egusphere-2026-3156
Preprint. Discussion started: 11 June 2026

vertical winds (black line) and the grey shaded area represent the remaining uncertainties in the measurements. The 15-minute vertical winds are approximately given by subtracting the uncertainty from the mean. The divergence-based vertical wind would be found in the grey shaded area above the mean. There is a factor 2 difference in the magnitude between the NMRC measurements and SE-WACCM-X, and another factor 2 can be found compared to JAWARA. These factors also hold for the heating/cooling rates.

The summer mesospheric cooling rate obtained from the measurements ranges from -40 to -100 K/d in the NMRC data. The winter heating rates are in the order of 5 to 35 K/d. The corresponding values for SE-WACCM-X and JAWARA scale with the corresponding differences of the vertical winds. Comparing the heating/cooling rates to trace gas data obtained from SABER reveals a rather good agreement in the magnitudes at similar altitudes. For the latitude of the NMRC, they found cooling rates during summer of -30 K/d at 90 km and -90/-100 K/d at 85 km altitude, respectively. In the winter season, heating rates of 20 to 50 K/d are derived. SABER CO_2 trace gases show comparable vertical velocities at the latitude of the NMRC, which results in rather similar heating and cooling rates. Furthermore, it is expected that the observations show larger vertical wind velocities. Models have a tendency to underestimate the vertical velocity at the smallest scales. These are the scales that often show the largest vertical motions (Chu, Xinzhao et al., 2026; Gudadze et al., 2019; Stober et al., 2018b). Another reason for the weaker maximum vertical velocities seems to be related to the much weaker meridional southward wind between 85-90 km in the NMRC observations compared to both models. In the following, we investigate the interyear variability and a potential connection between the meridional wind and the strength of the summer mesopause upwelling.

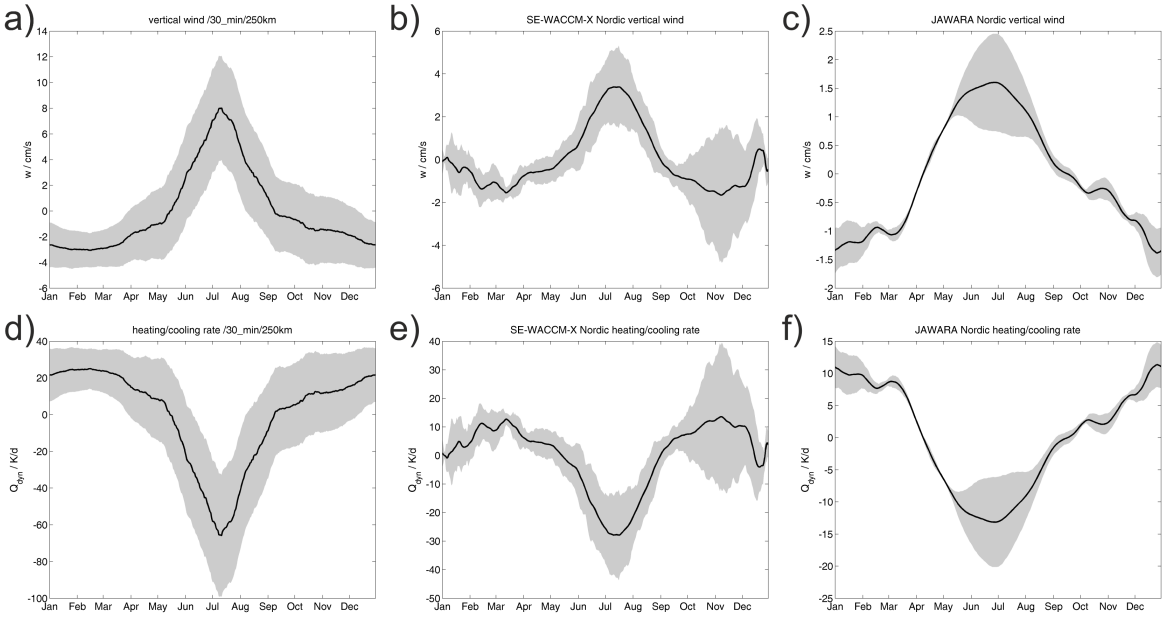

Figure 7. Vertical winds (top row) and heating/cooling rate(bottom row) for Nordic Meteor Radar Cluster with a 250 km diameter domain (left column), the free-running SE-WACCM-X (middle column), and the JAWARA reanalysis (right column).

https://doi.org/10.5194/egusphere-2026-3156
Preprint. Discussion started: 11 June 2026

6 Interyear variability of vertical winds

From 2021 through the end of 2025, the NMRC operated under mostly stable conditions with few major interruptions. Zonal, meridional, and vertical daily mean winds were calculated with the ASF2D (Baumgarten and Stober, 2019; Stober et al., 2020). A 30-day boxcar window was used to remove planetary waves. The hourly JAWARA reanalysis was injected into the same analysis pipeline to ensure optimal data preparation for a comparison of all wind components. The JAWARA data was reduced to the altitudes that match the coverage of the SVVP retrieval of the NMRC.

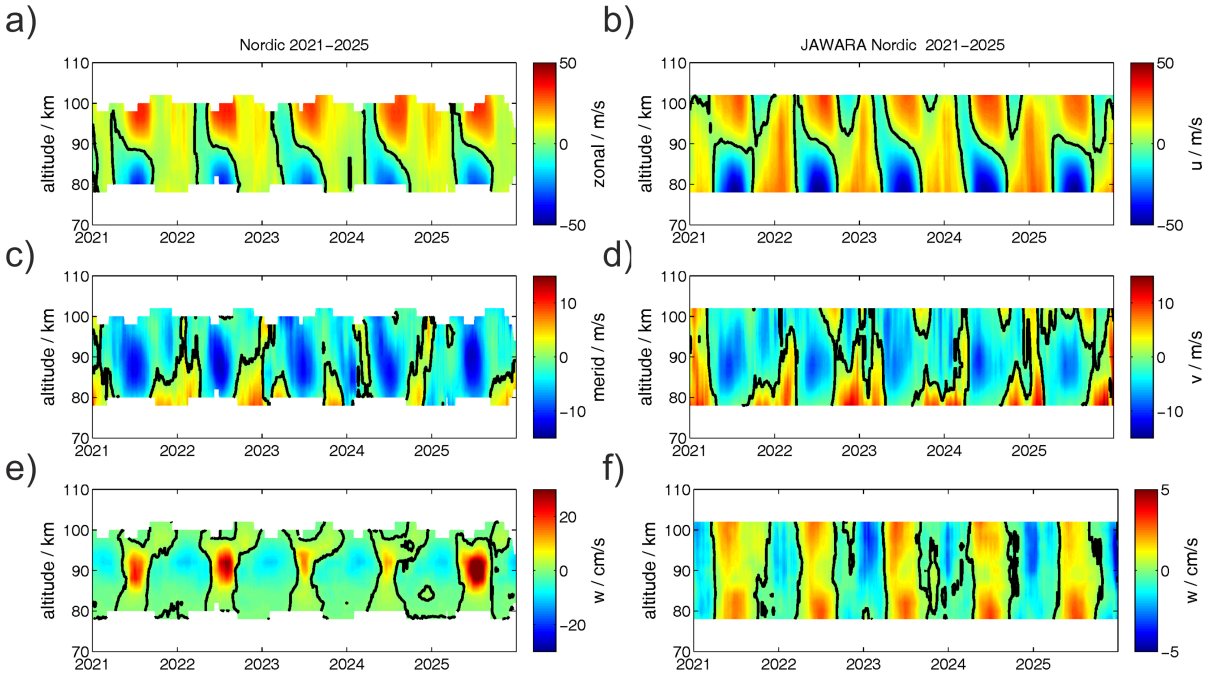

Figure 8. Comparison of horizontal and vertical winds between the Nordic Meteor Radar Cluster (left column, panels a), c), and e)), and the JAWARA reanalysis (right column, panels b), d), and f)).

In Figure 8, we show the obtained zonal, meridional, and vertical wind time series for NMRC (left column) and JAWARA (right column). The zero wind line for each wind component is highlighted by a black line. NMRC and JAWARA zonal mean winds reflect a very similar seasonal and interyear pattern. In particular, the summer wind reversal is well-reproduced in altitude and strength of eastward wind. JAWARA also captures the interyear differences of the spring transition above Fennoscandia. The most pronounced difference occurs in the wind magnitude, which is related to the winter polar vortex and summer westward jet in the mesosphere. JAWARA zonal winds are exceeding the mean values measured by the MRs. Meridional winds exhibit the same seasonal behaviour between JAWARA and the NMRC observations. During the winter season, JAWARA meridional northward winds are stronger than indicated by the measurements. JAWARA summer meridional

https://doi.org/10.5194/egusphere-2026-3156
Preprint. Discussion started: 11 June 2026

southward winds at altitudes between 80 and 95 km appear to be weaker in relation to the MR winds. Vertical winds are the most challenging parameter to estimate. The color scale was adapted to account for the different magnitudes in the vertical winds between the reanalysis and the measurements. JAWARA and NMRC vertical winds show very similar seasonal behaviour, with a summer upwelling for all altitudes and a corresponding hemispheric winter downwelling.

Previous comparisons of JAWARA at equatorial latitudes indicated a similar good agreement to observations of MLT winds (Sato et al., 2025). As JAWARA only assimilates temperatures, it was assumed that the effect of the Coriolis parameter plays a more important role at these low latitudes. Furthermore, data assimilation of wind measurements could further mitigate some of the existing differences between JAWARA and the NMRC observations.

7 Discussion

MLT (Mesosphere and Lower Thermosphere) vertical winds are among the most challenging dynamic parameters to measure. Previous studies utilizing various instruments, such as High Precision Large Aperture (HPLA) radars, have indicated the presence of downward vertical winds in the summer MLT (Fritts et al., 1990; Hoppe and Fritts, 1995b; Gudadze et al., 2019). In contrast, other measurement techniques, such as lidars, provide only short episodes of data, which makes it difficult to obtain climatologically reliable vertical wind measurements (Chu, Xinzhao et al., 2026). However, lidar observations are valuable due to the higher temporal resolution and small(tiny) sampling volume, providing thresholds of the small-scale and short-term variability. Although vertical winds derived from meteor radars have been reported previously (Egito et al., 2016; Chau et al., 2017), these measurements have shown extreme biases of several meters per second.

Multistatic meteor radar networks, such as the NMRC, permit the development of more sophisticated tomographic retrievals, which opened a path to retrieve vertical winds using different approaches to identify the nature of these biases and to reduce their impact (Stober et al., 2022). In this study, we present results using a newly developed SVVP method (Poku et al., 2026), which allowed us to retrieve vertical winds based on the direct Doppler measurement as well as by integrating the horizontal divergence. Both approaches resulted in a very similar seasonal structure and magnitude. The horizontal divergence-based winds tend to exceed the Doppler-based winds by 6-25%, which appears to be partly explainable by compressibility effects that are not taken into account yet. These compressibility effects can be significant. During the Hunga Tonga volcanic eruption, horizontal winds of more than 200 m/s were reported over the Andes (Qiao et al., 2025; Stober et al., 2023), which corresponds already to a transonic flow regime with even higher compressibility effects. Thus, the divergence-derived vertical winds present more of an upper limit of the magnitude, whereas the Doppler-based winds at the 15-minute level provide a lower threshold of the wind magnitude, due to the sparse measurement statistics. Previous studies using an MF radar to estimate the divergence between the measurement location and the South Pole resulted in a mean peak vertical wind velocity of 5 cm/s at 85 km altitude, which also falls in the range that we derived here (Vincent et al., 2019).

A crucial aspect of the presented vertical wind climatologies is the debiasing. The most precise vertical wind information from meteor radars is inferred by monitoring the meteor ablation altitude. This layer corresponds to a constant density surface (Stober et al., 2014; Dawkins et al., 2023, 2024). The altitude of this constant-density surface is a very reliable proxy of the vertical

https://doi.org/10.5194/egusphere-2026-3156
Preprint. Discussion started: 11 June 2026

motion at this height. Our de-basing is based on five years of data. The longer the time series, the more robust this approach gets.

JAWARA and SE-WACCM-X horizontal winds capture the observed seasonal pattern in both wind components. Zonal winds indicate a westward wind phase during the spring transition, eastward winds during hemispheric winter, and an asymmetric summer wind reversal during the summer months with a gradual descending reversal altitude. The winter season eastward winds due to the polar vortex appear to be stronger than shown by the observations in JAWARA as well as SE-WACCM-X. Meridional winds reflect a similar seasonal climatology with southward winds during the summer months and northward winds during the winter above Fennoscandia. However, the summer southward wind magnitude is stronger in the observations compared to both models. The improvement of the seaosnal climatologies for SE-WACCM-X (high-resolution, without gravity wave parameterization) compared to previous versions of WACCM-X(regular resolution, with gravity wave parameterization)is significant (Stober et al., 2021).

SE-WACCM-X vertical winds exhibit similar seasonal characteristics compared to the NMRC-derived winds. The magnitude of the summer upwelling almost matches the 15-minute retrieved observations. Only the altitude of the maximum summer wind upwelling appears to be lower by 7-10 km compared to the observations. JAWARA vertical winds indicate only a seasonal pattern with upwelling in summer and downwelling in winter. The magnitude is the smallest compared to the measurements and SE-WACCM-X, and shows no clear peak. Thus, the JAWARA vertical wind magnitude presents a lower limit of the summer upwelling. These seem to be expected considering the coarser spatial resolution of JAWARA compared to SE-WACCM-X and the measurements.

The derived heating/cooling rates reflect the variability and scaling of the vertical winds. NMRC obtained mesospheric summer/winter cooling/heating rates that seem to agree with the magnitude of SABER CO_2 based measurements (Yue and Wang, 2025) for the same latitude. These SABER trace gas measurements show vertical motions that correspond to 5-15 cm/s and, thus, fall within the model results of JAWARA, SE-WACCM-X, and our SVVP retrieved vertical winds, providing confidence that the measurements have the right order of magnitude.

Inter-year differences remain difficult to determine. JAWARA reanalysis depends on the stability of the data assimilation pipeline. Due to the end of the lifetime of the MLS instrument on board AURA, changes might emerge in the future. The quality of the reanalysis also depends on the available data products and their long-term stability. NMRC observations indicate some inter-year variability that appears to be connected to the strength of the southward winds around 90 km. However, as the Doppler-based vertical winds are only reliable around 90 km, a change of the maximum upwelling altitude might not be captured in our data, but still be included in the reanalysis, which provides a much more comprehensive picture. JAWARA horizontal winds capture some of the year-to-year changes that can be found above Fennoscandia, and the general seasonality remains preserved and consistent for all three wind components throughout the entire period.

https://doi.org/10.5194/egusphere-2026-3156
Preprint. Discussion started: 11 June 2026

8 Conclusions

Mesospheric vertical winds are still one of the most difficult atmospheric parameters to be observed. In this study, we present a comparison of vertical winds derived from a multistatic meteor radar network, the Nordic Meteor Radar Cluster. We performed a comprehensive analysis for a temporal resolution of 15- and 30-minute winds retrieved with a newly developed SVVP method. The implemented retrievals also permit the calculation of vertical winds by integrating the measured horizontal divergence. NMRC vertical winds showed a seasonally consistent pattern, and magnitudes ranged from 5 to 15 cm/s. The horizontal divergence-based winds represent an upper threshold and indicate almost no dependence on the temporal resolution. The Doppler analyzed vertical winds reflected some scaling effect due to lower measurement statistics for the 15-minute retrievals, attributed to the Tikhonov regularization. These winds represent the lower limit for the vertical upwelling during the hemispheric summer above Fennoscandia.

Horizontal winds measured with the NMRC exhibit a very good agreement with the horizontal wind climatologies derived from the meteorological reanalysis JAWARA and the free-running SE-WACCM-x. Both models capture the seasonal asymmetries in the zonal wind and also reproduce the seasonal structure of the meridional wind component. Vertical winds also reflect a similar seasonal climatology but with larger differences in the seasonal magnitudes of the summer upwelling and winter downwelling. SE-WACCM-X vertical winds are almost in agreement with the 15-minute SVVP retrievals. JAWARA winds are smaller by a factor of 2. However, the comparison provides constraints on the magnitude of the 'true' vertical wind, which likely is larger than the values from JAWARA and lower than the divergence-derived SVVP measurements.

NMRC estimated heating/cooling rates are in good agreement with the measurements observed from SABER and reach for the summer mesoscale region cooling rates from -40 to -100 K/d above Fennoscandia. During the hemispheric winter, heating rates from 5 to 20 K/d are derived from the SVVP retrievals. JAWARA and SE-WACCM-X indicate comparable lower values, which is expected as both models might not yet resolve the smallest gravity wave scales.

Compressibility effects appear to become important when deriving vertical winds from the horizontal divergence. Combining NMRC horizontal winds (diurnal peak values) and JAWARA temperatures resulted in Mach numbers close to 0.3 at the summer mesopause and for altitudes above 95 km, whereas the mean flow remains incompressible.

Author contributions. The SVVP algorithm was conceptualized through the ISSI International Team Meteors and Phenomena at the Boundary between Earth's Atmosphere and Outer Space, with leading roles of GS, AL, LP, WK, JZ, WY, and AK. SE-WACCM-X data simulation has been performed by HL; the data reduction was implemented by ZQ, HL, and GS. DJ, JZ, and WY provided auxiliary data from China and SAAMER-NOVA, essential for improving the SVVP implementation. MT, NG, SN, ML, JK, AK, and NM ensured the operation of the Nordic Meteor Radar Cluster. All authors contributed to the editing.

Competing interests. The authors have declared that they have no competing interests. However, Wen Yi is a member of the editorial board of Atmospheric Measurement Techniques.

https://doi.org/10.5194/egusphere-2026-3156
Preprint. Discussion started: 11 June 2026

Acknowledgements. Gunter Stober, Loretta Pearl Poku, and Witali Krochin are members of the Oeschger Center for Climate Change Research. Loretta Pearl Poku, Witali Krochin are supported by the Schweizerischer Nationalfonds zur Förderung der Wissenschaftlichen Forschung (grant no. 200021L-228107). Calculations were performed on UBELIX (http://www.id.unibe.ch/hpc, last access: 22. May 2026), the HPC cluster at the University of Bern. The development of the algorithm was motivated by the discussions of the International Space Science Institute (ISSI) in Bern, through the ISSI International Team Meteors and Phenomena at the Boundary between Earth's Atmosphere and Outer Space (project no. 23-580). Zishun Qiao acknowledges the U.S. NSF NCAR Advanced Study Program Postdoctoral Fellowship. Wen Yi is supported by the National Natural Science Foundation of China (Grants 42574213 and 42174183) and State Key Laboratory of Environment Characteristics and Effects for Near-space(No.2025NS02). Satonori Nozawa has been supported by the JSPS KAKENHI Grants, 21H04516, 21H04518, 23K20872, 23K28222, 24K00709, 24H00751, 25H00686, and 25H00696. The Esrange meteor radar operation, maintenance and data collection were provided by the SSC Space Esrange Space Center.

https://doi.org/10.5194/egusphere-2026-3156
Preprint. Discussion started: 11 June 2026

References

Amante, C. and Eakins, B. W.: ETOPO1 arc-minute global relief model: procedures, data sources and analysis, 2009.

Baumgarten, K. and Stober, G.: On the evaluation of the phase relation between temperature and wind tides based on ground-based measurements and reanalysis data in the middle atmosphere, Annales Geophysicae, 37, 581–602, https://doi.org/10.5194/angeo-37-581-2019, 2019.

Becker, E.: Dynamical Control of the Middle Atmosphere, Space Science Reviews, 168, 283–314, https://doi.org/10.1007/s11214-011-9841-5, 2012.

Chau, J. L., Stober, G., Hall, C. M., Tsutsumi, M., Laskar, F. I., and Hoffmann, P.: Polar mesospheric horizontal divergence and relative vorticity measurements using multiple specular meteor radars, Radio Science, pp. n/a–n/a, https://doi.org/10.1002/2016RS006225, 2016RS006225, 2017.

Chu, Xinzhao, Li, Xianxin, Jandreau, Jackson, and Chen, Yingfei: Vertical Wind Measurements with High-Resolution Lidars & Impacts on Antarctica Upper Atmosphere Studies, EPJ Web Conf., 362, 01 035, https://doi.org/10.1051/epjconf/202636201035, 2026.

Clemesha, B. and Batista, P.: The quantification of long-term atmospheric change via meteor ablation height measurements, Journal of Atmospheric and Solar-Terrestrial Physics, 68, 1934–1939, https://doi.org/https://doi.org/10.1016/j.jastp.2005.12.008, long-term Trends and Short-term Variability in the Upper, Middle and Lower Atmosphere, 2006.

Dawkins, E. C. M., Stober, G., Janches, D., Carrillo-Sánchez, J. D., Lieberman, R. S., Jacobi, C., Moffat-Griffin, T., Mitchell, N. J., Cobbett, N., Batista, P. P., Andrioli, V. F., Buriti, R. A., Murphy, D. J., Kero, J., Gulbrandsen, N., Tsutsumi, M., Kozlovsky, A., Kim, J. H., Lee, C., and Lester, M.: Solar Cycle and Long-Term Trends in the Observed Peak of the Meteor Altitude Distributions by Meteor Radars, Geophysical Research Letters, 50, e2022GL101 953, https://doi.org/https://doi.org/10.1029/2022GL101953, e2022GL101953 2022GL101953, 2023.

Dawkins, E. C. M., Janches, D., Stober, G., Carrillo-Sánchez, J. D., Lieberman, R. S., Jacobi, C., Moffat-Griffin, T., Mitchell, N. J., Cobbett, N., Batista, P. P., Andrioli, V. F., Buriti, R. A., Murphy, D. J., Kero, J., Gulbrandsen, N., Tsutsumi, M., Kozlovsky, A., Lester, M., Kim, J.-H., Lee, C., Liu, A., Fuller, B., O'Connor, D., Palo, S. E., Taylor, M. J., Marino, J., and Rainville, N.: Seasonal and Local Time Variation in the Observed Peak of the Meteor Altitude Distributions by Meteor Radars, Journal of Geophysical Research: Atmospheres, 129, e2024JD040 978, https://doi.org/https://doi.org/10.1029/2024JD040978, e2024JD040978 2024JD040978, 2024.

Egito, F., Andrioli, V., and Batista, P.: Vertical winds and momentum fluxes due to equatorial planetary scale waves using all-sky meteor radar over Brazilian region, Journal of Atmospheric and Solar-Terrestrial Physics, 149, 108 – 119, https://doi.org/https://doi.org/10.1016/j.jastp.2016.10.005, 2016.

Fritts, D. and Alexander, M. J.: Gravity wave dynamics and effects in the middle atmosphere, Reviews of Geophysics, 41, 1–64, https://doi.org/doi:10.1029/2001RG000106, 2003.

Fritts, D., Hoppe, U.-P., and Inhester, B.: A study of the vertical motion field near the high-latitude summer mesopause during MAC/SINE, Journal of Atmospheric and Terrestrial Physics, 52, 927–938, https://doi.org/https://doi.org/10.1016/0021-9169(90)90025-I, middle atmosphere dynamics at high latitudes, 1990.

Garcia, R. R., Smith, A. K., Kinnison, D. E., Álvaro de la Cámara, and Murphy, D. J.: Modification of the Gravity Wave Parameterization in the Whole Atmosphere Community Climate Model: Motivation and Results, Journal of the Atmospheric Sciences, 74, 275 – 291, https://doi.org/10.1175/JAS-D-16-0104.1, 2017.

https://doi.org/10.5194/egusphere-2026-3156
Preprint. Discussion started: 11 June 2026

Gelaro, R., McCarty, W., Suárez, M. J., Todling, R., Molod, A., Takacs, L., Randles, C. A., Darmenov, A., Bosilovich, M. G., Reichle, R., Wargan, K., Coy, L., Cullather, R., Draper, C., Akella, S., Buchard, V., Conaty, A., da Silva, A. M., Gu, W., Kim, G.-K., Koster, R., Lucchesi, R., Merkova, D., Nielsen, J. E., Partyka, G., Pawson, S., Putman, W., Rienecker, M., Schubert, S. D., Sienkiewicz, M., and Zhao, B.: The Modern-Era Retrospective Analysis for Research and Applications, Version 2 (MERRA-2), Journal of Climate, 30, 5419 – 5454, https://doi.org/10.1175/JCLI-D-16-0758.1, 2017.

Gudadze, N., Stober, G., and Chau, J. L.: Can VHF radars at polar latitudes measure mean vertical winds in the presence of PMSE?, Atmospheric Chemistry and Physics, 19, 4485–4497, https://doi.org/10.5194/acp-19-4485-2019, 2019.

Hindley, N. P., Mitchell, N. J., Cobbett, N., Smith, A. K., Fritts, D. C., Janches, D., Wright, C. J., and Moffat-Griffin, T.: Radar observations of winds, waves and tides in the mesosphere and lower thermosphere over South Georgia island (54° S, 36° W) and comparison with WACCM simulations, Atmospheric Chemistry and Physics, 22, 9435–9459, https://doi.org/10.5194/acp-22-9435-2022, 2022.

Hoppe, U.-P. and Fritts, D. C.: High-resolution measurements of vertical velocity with the European incoherent scatter VHF radar: 1. Motion field characteristics and measurement biases, Journal of Geophysical Research: Atmospheres, 100, 16 813–16 825, https://doi.org/https://doi.org/10.1029/95JD01466, 1995a.

Hoppe, U.-P. and Fritts, D. C.: On the downward bias in vertical velocity measurements by VHF radars, Geophysical Research Letters, 22, 619–622, https://doi.org/https://doi.org/10.1029/95GL00165, 1995b.

Koshin, D., Sato, K., Miyazaki, K., and Watanabe, S.: An ensemble Kalman filter data assimilation system for the whole neutral atmosphere, Geoscientific Model Development, 13, 3145–3177, https://doi.org/10.5194/gmd-13-3145-2020, 2020.

Koshin, D., Sato, K., Kohma, M., and Watanabe, S.: An update on the 4D-LETKF data assimilation system for the whole neutral atmosphere, Geoscientific Model Development, 15, 2293–2307, https://doi.org/10.5194/gmd-15-2293-2022, 2022.

Koshin, D., Sato, K., Watanabe, S., and Miyazaki, K.: The JAGUAR-DAS whole neutral atmosphere reanalysis: JAWARA, Prog Earth Planet Sci, 12, https://doi.org/10.1186/s40645-024-00674-3, 2025.

Lauritzen, P. H., Nair, R. D., Herrington, A. R., Callaghan, P., Goldhaber, S., Dennis, J. M., Bacmeister, J. T., Eaton, B. E., Zarzycki, C. M., Taylor, M. A., Ullrich, P. A., Dubos, T., Gettelman, A., Neale, R. B., Dobbins, B., Reed, K. A., Hannay, C., Medeiros, B., Benedict, J. J., and Tribbia, J. J.: NCAR Release of CAM-SE in CESM2.0: A Reformulation of the Spectral Element Dynamical Core in Dry-Mass Vertical Coordinates With Comprehensive Treatment of Condensates and Energy, Journal of Advances in Modeling Earth Systems, 10, 1537–1570, https://doi.org/https://doi.org/10.1029/2017MS001257, 2018.

Lindzen, R. S.: Turbulence and stress owing to gravity wave and tidal breakdown, Journal of Geophysical Research: Oceans, 86, 9707–9714, https://doi.org/10.1029/JC086iC10p09707, 1981.

Liu, H.-L.: Transport of Nitric Oxide in the Winter Mesosphere and Lower Thermosphere, Geophysical Research Letters, 52, e2024GL113 027, https://doi.org/https://doi.org/10.1029/2024GL113027, e2024GL113027 2024GL113027, 2025.

Liu, H.-L., Bardeen, C. G., Foster, B. T., Lauritzen, P., Liu, J., Lu, G., Marsh, D. R., Maute, A., McInerney, J. M., Pedatella, N. M., Qian, L., Richmond, A. D., Roble, R. G., Solomon, S. C., Vitt, F. M., and Wang, W.: Development and Validation of the Whole Atmosphere Community Climate Model With Thermosphere and Ionosphere Extension (WACCM-X 2.0), Journal of Advances in Modeling Earth Systems, 10, 381–402, https://doi.org/https://doi.org/10.1002/2017MS001232, 2018.

Liu, H.-L., Lauritzen, P. H., Vitt, F., and Goldhaber, S.: Assessment of Gravity Waves From Tropopause to Thermosphere and Ionosphere in High-Resolution WACCM-X Simulations, Journal of Advances in Modeling Earth Systems, 16, e2023MS004 024, https://doi.org/https://doi.org/10.1029/2023MS004024, e2023MS004024 2023MS004024, 2024.

https://doi.org/10.5194/egusphere-2026-3156
Preprint. Discussion started: 11 June 2026

McCormack, J. P., Harvey, V. L., Randall, C. E., Pedatella, N., Koshin, D., Sato, K., Coy, L., Watanabe, S., Sassi, F., and Holt, L. A.: Intercomparison of middle atmospheric meteorological analyses for the Northern Hemisphere winter 2009–2010, Atmospheric Chemistry and Physics, 21, 17 577–17 605, https://doi.org/10.5194/acp-21-17577-2021, 2021.

McFarlane, N. A.: The Effect of Orographically Excited Gravity Wave Drag on the General Circulation of the Lower Stratosphere and Troposphere, Journal of Atmospheric Sciences, 44, 1775 – 1800, https://doi.org/10.1175/1520-0469(1987)044<1775:TEOOEG>2.0.CO;2, 1987.

Poku, L. P., Stober, G., Krochin, W., Liu, A., Kozlovsky, A., Janches, D., Zeng, J., Yi, W., Tsutsumi, M., Gulbrandsen, N., Nozawa, S., Lester, M., Kero, J., and Mitchell, N.: Comparison of tomographic wind retrievals with different geometric implementations for multistatic meteor radar networks, EGUsphere, 2026, 1–32, https://doi.org/10.5194/egusphere-2025-6377, 2026.

Qiao, Z., Liu, A. Z., Stober, G., Fuentes, J., Vargas, F., Adami, C. L., and Reid, I. M.: Chilean Observation Network De Meteor Radars (CONDOR): multi-static system configuration and wind comparison with co-located lidar, Atmospheric Measurement Techniques, 18, 1091–1104, https://doi.org/10.5194/amt-18-1091-2025, 2025.

Richter, J. H., Sassi, F., and Garcia, R. R.: Toward a Physically Based Gravity Wave Source Parameterization in a General Circulation Model, Journal of the Atmospheric Sciences, 67, 136 – 156, https://doi.org/10.1175/2009JAS3112.1, 2010.

Rodgers, C. D.: Inverse Methods for Atmospheric Sounding: Theory and Practice, Singapore: World Scientific, 2000.

Sato, K. and Koshin, D.: JAGUAR Data Assimilation System Whole neutral Atmosphere Reanalysis (JAWARA) [Data set]., https://doi.org/https://doi.org/10.17592/002.2025010407, 2025.

Sato, K., Tsutsumi, M., Sato, T., Nakamura, T., Saito, A., Tomikawa, Y., Nishimura, K., Kohma, M., Yamagishi, H., and Yamanouchi, T.: Program of the Antarctic Syowa MST/IS radar (PANSY), Journal of Atmospheric and Solar-Terrestrial Physics, 118, 2–15, https://doi.org/https://doi.org/10.1016/j.jastp.2013.08.022, recent progress from networked studies based around MST radar, 2014.

Sato, K., Kohma, M., Tsutsumi, M., and Sato, T.: Frequency spectra and vertical profiles of wind fluctuations in the summer Antarctic mesosphere revealed by MST radar observations, Journal of Geophysical Research: Atmospheres, 122, 3–19, https://doi.org/https://doi.org/10.1002/2016JD025834, 2017.

Sato, K., Tomikawa, Y., Kohma, M., Yasui, R., Koshin, D., Okui, H., Watanabe, S., Miyazaki, K., Tsutsumi, M., Murphy, D., Meek, C., Tian, Y., Ern, M., Baumgarten, G., Chau, J. L., Chu, X., Collins, R., Espy, P. J., Hashiguchi, H., Kavanagh, A. J., Latteck, R., Lübken, F.-J., Milla, M., Nozawa, S., Ogawa, Y., Shiokawa, K., Alexander, M. J., Nakamura, T., and Ward, W. E.: Interhemispheric Coupling Study by Observations and Modelling (ICSOM): Concept, Campaigns, and Initial Results, Journal of Geophysical Research: Atmospheres, 128, e2022JD038 249, https://doi.org/https://doi.org/10.1029/2022JD038249, e2022JD038249 2022JD038249, 2023.

Sato, K., Koshin, D., Suclupe, J., Chau, J. L., Lima, L. M., Li, G., Bhaskara Rao, S. V., Ratnam, M. V., Rodriguez, R., and Scipion, D.: Causes of the Abnormally Strong Easterly Phase of the Mesopause Semiannual Oscillation During the March Equinox of 2023 Revealed by a New Reanalysis Data Covering the Entire Middle Atmosphere, Geophysical Research Letters, 52, e2025GL114 658, https://doi.org/https://doi.org/10.1029/2025GL114658, e2025GL114658 2025GL114658, 2025.

Smith, A. K.: Global Dynamics of the MLT, Surveys in Geophysics, 33, 1177–1230, https://doi.org/10.1007/s10712-012-9196-9, 2012.

Sommer, S., Stober, G., and Chau, J. L.: On the angular dependence and scattering model of polar mesospheric summer echoes at VHF, Journal of Geophysical Research: Atmospheres, 121, 278–288, https://doi.org/https://doi.org/10.1002/2015JD023518, 2016.

Stober, G., Matthias, V., Brown, P., and Chau, J. L.: Neutral density variation from specular meteor echo observations spanning one solar cycle, Geophysical Research Letters, 41, 6919–6925, https://doi.org/https://doi.org/10.1002/2014GL061273, 2014.

https://doi.org/10.5194/egusphere-2026-3156
Preprint. Discussion started: 11 June 2026

Stober, G., Chau, J. L., Vierinen, J., Jacobi, C., and Wilhelm, S.: Retrieving horizontally resolved wind fields using multi-static meteor radar observations, Atmospheric Measurement Techniques, 11, 4891–4907, https://doi.org/10.5194/amt-11-4891-2018, 2018a.

Stober, G., Sommer, S., Schult, C., Latteck, R., and Chau, J. L.: Observation of Kelvin–Helmholtz instabilities and gravity waves in the summer mesopause above Andenes in Northern Norway, Atmospheric Chemistry and Physics, 18, 6721–6732, https://doi.org/10.5194/acp-18-6721-2018, 2018b.

Stober, G., Baumgarten, K., McCormack, J. P., Brown, P., and Czarnecki, J.: Comparative study between ground-based observations and NAVGEM-HA analysis data in the mesosphere and lower thermosphere region, Atmospheric Chemistry and Physics, 20, 11 979–12 010, https://doi.org/10.5194/acp-20-11979-2020, 2020.

Stober, G., Kuchar, A., Pokhotelov, D., Liu, H., Liu, H.-L., Schmidt, H., Jacobi, C., Baumgarten, K., Brown, P., Janches, D., Murphy, D., Kozlovsky, A., Lester, M., Belova, E., Kero, J., and Mitchell, N.: Interhemispheric differences of mesosphere–lower thermosphere winds and tides investigated from three whole-atmosphere models and meteor radar observations, Atmospheric Chemistry and Physics, 21, 13 855–13 902, https://doi.org/10.5194/acp-21-13855-2021, 2021.

Stober, G., Liu, A., Kozlovsky, A., Qiao, Z., Kuchar, A., Jacobi, C., Meek, C., Janches, D., Liu, G., Tsutsumi, M., Gulbrandsen, N., Nozawa, S., Lester, M., Belova, E., Kero, J., and Mitchell, N.: Meteor radar vertical wind observation biases and mathematical debiasing strategies including the 3DVAR+DIV algorithm, Atmospheric Measurement Techniques, 15, 5769–5792, https://doi.org/10.5194/amt-15-5769-2022, 2022.

Stober, G., Liu, A., Kozlovsky, A., Qiao, Z., Krochin, W., Shi, G., Kero, J., Tsutsumi, M., Gulbrandsen, N., Nozawa, S., Lester, M., Baumgarten, K., Belova, E., and Mitchell, N.: Identifying gravity waves launched by the Hunga Tonga–Hunga Ha'apai volcanic eruption in mesosphere/lower-thermosphere winds derived from CONDOR and the Nordic Meteor Radar Cluster, Annales Geophysicae, 41, 197–208, https://doi.org/10.5194/angeo-41-197-2023, 2023.

Vadas, S. L.: Compressible f-plane solutions to body forces, heatings, and coolings, and application to the primary and secondary gravity waves generated by a deep convective plume, Journal of Geophysical Research: Space Physics, 118, 2377–2397, https://doi.org/https://doi.org/10.1002/jgra.50163, 2013.

Vadas, S. L., Zhao, J., Chu, X., and Becker, E.: The Excitation of Secondary Gravity Waves From Local Body Forces: Theory and Observation, Journal of Geophysical Research: Atmospheres, 123, 9296–9325, https://doi.org/10.1029/2017JD027970, 2018.

Vincent, R. A., Kovalam, S., Murphy, D. J., Reid, I. M., and Younger, J. P.: Trends and Variability in Vertical Winds in the Southern Hemisphere Summer Polar Mesosphere and Lower Thermosphere, Journal of Geophysical Research: Atmospheres, 124, 11 070–11 085, https://doi.org/https://doi.org/10.1029/2019JD030735, 2019.

Yi, W., Xue, X., Reid, I. M., Younger, J. P., Chen, J., Chen, T., and Li, N.: Estimation of Mesospheric Densities at Low Latitudes Using the Kunming Meteor Radar Together With SABER Temperatures, Journal of Geophysical Research: Space Physics, 123, 3183–3195, https://doi.org/https://doi.org/10.1002/2017JA025059, 2018.

Yue, J. and Wang, N.: Estimation of adiabatic cooling and warming in the mesosphere and lower thermosphere, Journal of Atmospheric and Solar-Terrestrial Physics, 269, 106 492, https://doi.org/https://doi.org/10.1016/j.jastp.2025.106492, 2025.

Zeng, J., Yi, W., Xue, X., Reid, I., Hao, X., Li, N., Chen, J., Chen, T., and Dou, X.: Comparison between the Mesospheric Winds Observed by Two Collocated Meteor Radars at Low Latitudes, Remote Sensing, 14, https://doi.org/10.3390/rs14102354, 2022.